



Cite this: *Chem. Commun.*, 2024, 60, 5984

Received 1st April 2024,  
Accepted 13th May 2024

DOI: 10.1039/d4cc01484g

rsc.li/chemcomm

# Rational design of pH-responsive near-infrared spirocyclic cyanines: the effects of substituents and the external environment†

Akihiro Sakama,<sup>ib</sup> ‡<sup>a</sup> Hyemin Seo,<sup>‡</sup><sup>a</sup> Joji Hara,<sup>a</sup> Yutaka Shindo,<sup>bc</sup> Yuma Ikeda,<sup>a</sup> Kotaro Oka,<sup>bcd</sup> Daniel Citterio<sup>ib</sup><sup>a</sup> and Yuki Hiruta<sup>ib</sup> \*<sup>a</sup>

**pH-responsive spirocyclic cyanine dyes were designed and synthesized. The equilibrium constant for cyclization ( $pK_{\text{cycl}}$ ) could be rationally controlled by changing the nucleophilic moiety and the side chains. Encapsulation in polymeric micelles inhibited the H-aggregation of the dye, and the  $pK_{\text{cycl}}$  could be shifted according to the amphiphilic polymer employed.**

Fluorescent dyes have been gaining much attention in the field of bioimaging due to their high brightness and biocompatibility. While autofluorescence and high background signals are conventional drawbacks of fluorescence imaging, it is effective to use fluorescence in the near-infrared (NIR,  $\lambda = 650\text{--}900\text{ nm}$ ) region to selectively visualize the target tissue, while suppressing autofluorescence from normal tissue, especially in *in vivo* deep tissue imaging.<sup>1</sup> Although several types of NIR fluorescent dyes have been developed as bioimaging probes, most of them could not differentiate the target cells or tissue from normal ones or blood vessels. This issue can be overcome by imparting responsiveness to a stimulus, such as pH change, to the dyes. The pH level in a living organism is strictly controlled and is closely related to biological functions. Therefore, the difference in pH provides clues for understanding biological phenomena and diagnosing diseases.<sup>2</sup> pH-responsive fluorescent probes

emitting visible light have been developed based on xanthene or boron dipyrromethene scaffolds;<sup>3,4</sup> however, only limited examples of pH-responsive NIR probes have been reported.

Heptamethine cyanines are NIR fluorescent dyes known to possess high potential for cancer imaging. Indocyanine green (ICG) has been approved for clinical use in sentinel lymph node (SLN) mapping during surgery due to its low toxicity.<sup>5</sup> One limitation of ICG is its short imaging time because of its poor stability. IR-780, another popular heptamethine cyanine dye, has improved fluorescence properties compared with ICG and long retention time for *in vivo* imaging,<sup>6</sup> and has great potential as a bioimaging agent. However, most heptamethine cyanine dyes lack targetability to the cells/tissues of interest. Attempts have been made to add sensing ability to cyanine dyes. Among them, pH-responsive cyanines have been actively investigated. One of them possesses a basic nitrogen atom in the dye structure. Cyanines lacking side chains on one or both indole-nine nitrogen atoms exhibit long-wavelength absorption and fluorescence under acidic conditions, while under basic conditions the absorption shifts to shorter wavelengths and little fluorescence is emitted.<sup>7</sup> The weak point of this type of pH-responsive cyanines is the difficulty in finely adjusting the range of pH response according to the target pH. Aminocyanine derivatives bearing a diamine moiety on the central carbon of the polymethine chain were developed.<sup>8,9</sup> Fluorescence quenching by photo-induced electron transfer (PeT) has also been employed for controlling the fluorescence of heptamethine cyanines.<sup>10</sup> However, the highest occupied molecular orbital (HOMO) level of NIR dyes is rather high for sufficient fluorescence quenching by PeT.<sup>11</sup> Lin's group and Miki's group had their eye on spirocyclization as the mechanism for pH-responsive ON/OFF switching of the fluorescence. They designed heptamethine cyanines bearing a nucleophilic moiety, which causes nucleophilic attack to the electron-deficient polymethine chain to form a cycle (spirocyclization).<sup>12,13</sup> Xie and co-workers also developed fluorescent pH turn-on oxazinoindoline dyes utilizing spirocyclization.<sup>14</sup> Spirocyclization has been applied mainly to fluorescein and rhodamine derivatives.<sup>15,16</sup> The conversion between

<sup>a</sup> Department of Applied Chemistry, Faculty of Science and Technology, Keio University, Hiyoshi 3-14-1, Kohoku-ku, Yokohama, Kanagawa, 223-8522, Japan. E-mail: hiruta@applc.keio.ac.jp

<sup>b</sup> Department of Biosciences and Informatics, Faculty of Science and Technology, Keio University, 3-14-1 Hiyoshi, Kohoku-ku, Yokohama, Kanagawa 223-8522, Japan

<sup>c</sup> School of Frontier Engineering, Kitasato University, 1-15-1 Kitasato, Minami-ku, Sagami-hara, Kanagawa, 252-0373, Japan

<sup>d</sup> Waseda Research Institute for Science and Engineering, Waseda University, 2-2 Wakamatsu-cho, Shinjuku-ku, Tokyo 162-8480, Japan

<sup>e</sup> College of Medicine, Kaohsiung Medical University, Kaohsiung City 80708, Taiwan

† Electronic supplementary information (ESI) available: Experimental procedures, absorption and fluorescence spectra, and <sup>1</sup>H and <sup>13</sup>C NMR spectra of the new compounds. See DOI: <https://doi.org/10.1039/d4cc01484g>

‡ A. S. and H. S. contributed equally.



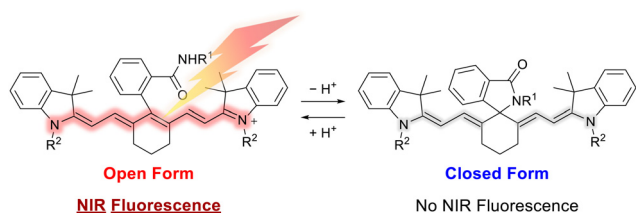


**Fig. 1** Molecular design strategy for pH-responsive cyanine dye: the closed form is converted to the open form *via* protonation.

open and closed forms causes a drastic change in the conjugated system, connecting and breaking up, resulting in a large change in absorbance and an associated distinct OFF/ON change in fluorescence. The value of the equilibrium constant between the open and closed form of the dye ( $pK_{\text{cycl}}$ ) is dependent on the structure of the nucleophilic moiety and the electron density of the fluorophore;<sup>17,18</sup> thus, the pH response range can be tuned according to the purpose. However, there are few previous reports revealing a relationship between  $pK_{\text{cycl}}$  and the structure of heptamethine cyanine dyes.

We decided to clarify how  $pK_{\text{cycl}}$  is altered by changing the nucleophilic moiety and the hydrophobicity of a spirocyclic cyanine, and the environment in which the dye is placed. In this context, we synthesized pH-responsive spirocyclic cyanine dyes having hydroxymethyl, methylcarbamoyl, or arylcarbamoyl groups as the nucleophilic subunit (Fig. 1). To evaluate the effect of the hydrophobicity of the dye on  $pK_{\text{cycl}}$ , several substituents with different polarity were introduced into the side chains on the indolenine nitrogens.

Heptamethine cyanine dyes can generally easily undergo self-aggregation due to the wide  $\pi$ -conjugated system. Encapsulation with lipids or micelles can prevent self-aggregation and improve the photostability, biocompatibility, fluorescence intensity, and water-solubility.<sup>19</sup> In this work, the dyes were encapsulated into polymeric micelles, and their pH responsiveness in the encapsulated environment was evaluated.

A spirocyclic cyanine dye with a hydroxymethyl group (**IR-HM**) was firstly synthesized (Fig. 2a), because the hydroxymethyl group has been frequently employed in previously reported spirocyclic dyes such as rhodamine derivatives, and **IR-HM** can be synthesized by a single step from commercially available IR-780. To evaluate the pH responsiveness of **IR-HM**, absorption and fluorescence spectra (Fig. S2a and d in the ESI†) were measured at different pH.

At pH 9.0, **IR-HM** has an absorption peak at 761 nm and the fluorescence emission peak was measured to be at 785 nm, which is also in the NIR region. **IR-HM** should exist solely as the open form at this pH. On the other hand, the absorption peak shifted to 400 nm in basic environments (pH 12.5), and there was almost no absorbance at 760 nm, resulting in a 360 nm shift from the NIR to the UV region, which indicated that a spirocyclization reaction occurred. As the case of the rhodamine derivative shows, spirocyclization causes such a dramatic absorption change that the dye changes from colorless to colored. The interruption/connection of the central conjugated

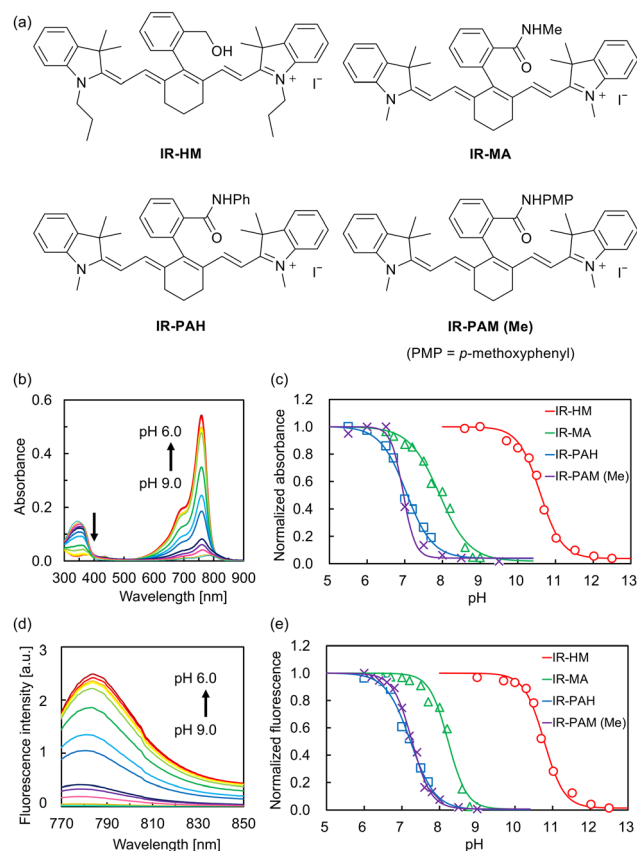


**Fig. 2** (a) Molecular structures of pH-responsive cyanine dyes. (b) Absorption spectra of **IR-PAM (Me)** (4  $\mu\text{M}$  dye in 25 mM buffer solution containing 10% DMSO). (c) Comparison of pH-responsive change in normalized absorbance of **IR-HM**, **IR-MA**, **IR-PAH**, and **IR-PAM (Me)** at maximum wavelength (761, 757, 760, 759 nm, respectively). (d) Fluorescence emission spectra of **IR-PAM (Me)** (4  $\mu\text{M}$  dye in 25 mM buffer solution containing 10% DMSO,  $\lambda_{\text{ex}}$  = 740 nm). (e) Comparison of pH-responsive change in normalized fluorescence intensity of **IR-HM**, **IR-MA**, **IR-PAH**, and **IR-PAM (Me)** at maximum wavelength (785, 784, 785, 784 nm, respectively,  $\lambda_{\text{ex}}$  = 740 nm).

chain upon cyclization/ring opening equilibrium causes a large shift in absorption wavelength, and more drastic OFF/ON switching of the fluorescence in the NIR region is achieved, compared with pH-responsive cyanine dyes based on simple protonation equilibrium.<sup>7–9</sup> The structural change upon the spirocyclization equilibrium was reflected also in the chemical shifts in the  $^1\text{H}$  NMR spectra and the appearance of the sample solutions (Fig. S3 in the ESI†). Additionally, the quantum chemical calculations of frontier orbital energy levels confirmed the change in the HOMO–LUMO energy gap depending on the spirocyclization equilibrium (Fig. S4 in the ESI†). The molecular design of spirocyclic dyes using a hydroxymethyl group was confirmed to be applicable to cyanine dyes and to provide a sharp pH response. However, the  $pK_{\text{cycl}}$  [10.6/10.8, determined based on absorbance (Abs) and fluorescence intensity (FI), respectively] was too high for the dye to work in the physiological pH range (Fig. 2c and e), so it was necessary to change the nucleophilic moiety. It was previously reported that unsubstituted carbamoyl groups are applicable as the



nucleophile for spirocyclic heptamethine cyanine dyes and provide a pH-responsive change in fluorescence intensity in the broad range of pH 4–11.<sup>12</sup> We designed a cyanine dye possessing a methylcarbamoyl group (**IR-MA**), aiming at enhancement of the nucleophilicity of the carbamoyl group by an electron-donating methyl group (Fig. 2a). Its  $pK_{\text{cycl}}$  was successfully lowered to 7.9 (Abs)/8.2 (FI) (Fig. S2b, e in the ESI† and Fig. 2c, e). By installing a more acidic phenyl amide<sup>20</sup> moiety [**IR-PAH** and **IR-PAM (Me)**] as shown in Fig. 2a, the  $pK_{\text{cycl}}$  was further shifted to 7.0 (Abs)/7.2 (FI) and 7.1 (Abs)/7.3 (FI), respectively (Fig. S2c, f in the ESI† and Fig. 2b–e).

IR-PAM derivatives were chosen to evaluate the effect of the side chains on  $pK_{\text{cycl}}$ . To increase the water solubility of **IR-PAM (Me)**, IR-PAM with carboxylic acid moieties [**IR-PAM (COOH)**] and its PEG amide [**IR-PAM (PEG)**] were synthesized (Fig. 3a). Their  $pK_{\text{cycl}}$  values were determined to be 10.9 (Abs)/11.2 (FI) and 10.2 (Abs)/10.8 (FI), respectively, larger than those of **IR-PAM (Me)** (Fig. S5a, b, e, f in the ESI† and Fig. 3b). Conversely, when introducing hydrophobic substituents [**IR-PAM (COOt-Bu)** and **IR-PAM (n-Hex)**], as shown in Fig. 3a, the  $pK_{\text{cycl}}$  shifted to the acidic side (Fig. S5c, d, g, h in the ESI† and Fig. 3b). This demonstrates that the dye with a more hydrophilic chromophore part has a higher  $pK_{\text{cycl}}$ . In other words, the open form of the hydrophilic dye is more stable than that of the hydrophobic dye in aqueous solution of the same pH. As the open form is positively charged, it is stabilized by hydration, and polar substituents increase the energetic gain by hydration. On the other hand, hydrophobic substituents hinder hydration of the dye, decreasing the stability of the open form.

Judging from the shape of the absorbance spectra (Fig. S3c and d in the ESI†), the dyes with hydrophobic substituents were considered

to form H-aggregates, which results in a shorter peak wavelength than the original maximum wavelength of the dyes ( $\sim 760$  nm). To prevent H-aggregation, **IR-PAM (n-Hex)** was encapsulated in amphiphilic polymeric micelles (Fig. S6 in the ESI†). Pluronic F127 (PEG-PPO-PEG) and PEG-*b*-PCL were employed as polymers because of their high biocompatibility. The center of those amphiphilic polymeric micelles has a hydrophobic core coated by a hydrophilic shell, and hence hydrophobic dyes would be localized in the hydrophobic core. The encapsulation efficiency of **IR-PAM (n-Hex)@F127** was 95.8%. The absorption spectra of **IR-PAM (n-Hex)@F127** were measured, and less H-aggregate peaks were observed (Fig. 4a). This result indicates that the aggregation was prevented by encapsulation. A pH-responsive change in absorbance was also observed. Fluorescence intensity increased from pH 8.5 to 5.8 as the pH was lowered, but decreased below pH 5.5 (Fig. 4b). This is considered to be caused by the inner filter effect, in which the emitted fluorescence is absorbed by the surrounding dye molecules and quenched, due to the high concentration of dye in the micelle. The  $pK_{\text{cycl}}$  of **IR-PAM (n-Hex)@PEG-*b*-PCL** was located on the more basic side compared to that of **IR-PAM (n-Hex)@F127** [8.1 (Abs)/8.3 (FI) and 6.2 (Abs)/6.8 (FI), respectively] as shown in Fig. S7 in the ESI† and Fig. 4c and d. This is because PEG-*b*-PCL micelles have a more hydrophobic core than F127, based on the evaluation of the polarity of the core of each

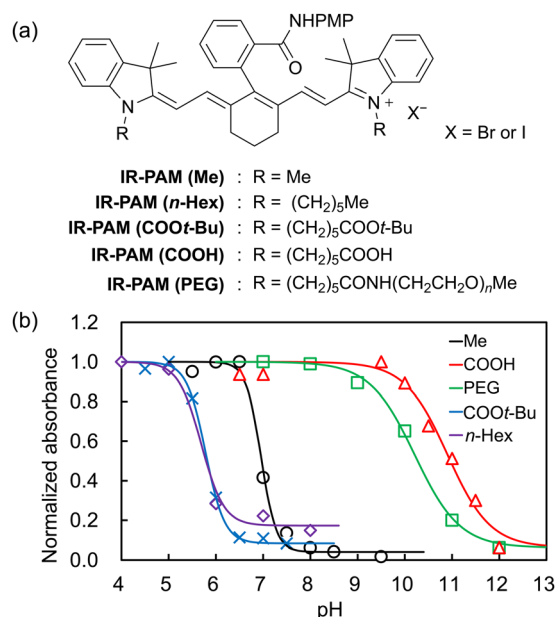


Fig. 3 (a) Molecular structures of IR-PAM derivatives. (b) Comparison of pH-responsive change in normalized absorbance of IR-PAM derivatives at maximum wavelength [759 nm (Me), 766 nm (COOH), 767 nm (PEG), 774 nm (COOt-Bu), 765 nm (n-Hex)].

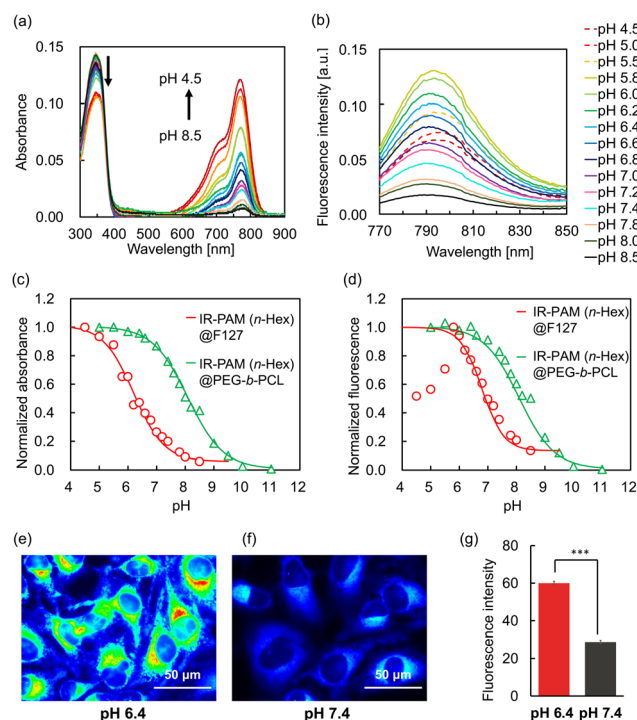


Fig. 4 (a) Absorption and (b) fluorescence emission spectra of **IR-PAM (n-Hex)@F127** (2  $\mu\text{M}$  dye). (c) Normalized absorbance of **IR-PAM (n-Hex)@F127** and **IR-PAM (n-Hex)@PEG-*b*-PCL** at maximum wavelength (771, 773 nm, respectively). (d) Normalized fluorescence intensity of **IR-PAM (n-Hex)@F127** and **IR-PAM (n-Hex)@PEG-*b*-PCL** at maximum wavelength (792, 793 nm, respectively). Fluorescence images of HeLa cells stained with **IR-PAM(n-Hex)@F127** at (e) pH 6.4 and (f) pH 7.4. (g) Comparison of fluorescence intensity of (e) and (f). \*\*\* $p < 0.001$ .



micelle using the solvatofluorochromic dye KSD-3<sup>21</sup> (Fig. S8 in the ESI†). The more hydrophobic the environment of the dye, the more stably the dye can exist as the open form, which explains the shift of  $pK_{\text{cycl}}$  towards the basic side. The response curves obtained using either type of polymeric micelles exhibited a wider pH-response range compared to those observed in the aqueous solution of the dye alone. This finding is consistent with prior reports indicating that within polymeric micelles, the dyes exhibited multiple apparent  $pK_a$  values depending on their localization (from the center of the core to the interface with the aqueous solution), thus resulting in a broad pH-response range.<sup>22,23</sup>

Since we succeeded in developing pH-responsive cyanine dye-encapsulated polymeric micelles that work in the physiological pH range, their application to cellular pH imaging was investigated. The extracellular pH of cancer cells is around 6.5 and shows a rather acidic environment compared with normal cells (pH 7.4).<sup>24</sup> To evaluate the applicability of **IR-PAM (n-Hex)@F127** to visualize an acidic environment, we incubated HeLa cells, whose intracellular pH was intentionally changed to pH 6.4 and 7.4 by using nigericin, with **IR-PAM (n-Hex)@F127** (Fig. 4e and f). The measured fluorescence intensities at pH 6.4 were approximately twice as high as those at pH 7.4 (Fig. 4g). **IR-PAM (n-Hex)@F127** appeared to be mainly localized to the lipid membranes of organelles, and its localization did not change with pH. Thus, it can be concluded that **IR-PAM (n-Hex)@F127** is applicable for NIR fluorescence imaging of cell acidity.

In summary, we have developed spirocyclic cyanine dyes, and demonstrated that changing their chemical structure resulted in a different pH response. By changing the nucleophile moiety from a hydroxy group (**IR-HM**) to an amide moiety [**IR-MA**, **IR-PAH** and **IR-PAM (Me)**], the  $pK_{\text{cycl}}$  was lowered from 11 to around 7–8. Next, **IR-PAM (COOH)**, **IR-PAM (PEG)**, **IR-PAM (COOt-Bu)**, and **IR-PAM (n-Hex)** were synthesized, and the effect of the polarity of the side chains on  $pK_{\text{cycl}}$  was evaluated. The pH-responsiveness of these derivatives showed that a more hydrophilic dye structure leads to an increase in the  $pK_{\text{cycl}}$ . **IR-PAM (n-Hex)** was encapsulated into amphiphilic polymers to suppress the aggregation and improve the solubility in water. The  $pK_{\text{cycl}}$  of **IR-PAM (n-Hex)** in the micelles shifted to reflect the hydrophobicity of the polymer chain. NIR laser irradiation of HeLa cells stained with **IR-PAM (n-Hex)@F127** showed a 2-fold difference in fluorescence emission at intracellular pH of 6.4 and 7.4. Thus, we demonstrated the effects of substituents and the external environment on the pH-responsiveness of spirocyclic cyanine dyes and provided guidelines for the regulation of it. Through further sensitization of pH response and tuning of  $pK_{\text{cycl}}$ , these spirocyclic cyanines will offer potential applications for *in vivo* imaging or biomedical tools, such as cancer diagnosis and photothermal therapy.

Akihiro Sakama: formal analysis, writing – original draft. Hyemin Seo: investigation, writing – original draft. Joji Hara: investigation. Yutaka Shindo: investigation. Yuma Ikeda: investigation. Kotaro Oka: supervision, resources. Daniel Citterio: writing – review & editing, supervision. Yuki Hiruta: conceptualization, methodology, writing – review & editing, supervision, project administration, funding acquisition.

This study was supported by Grant-in Aid for Early-Career Scientists (Grant no. 19K16339), and Scientific Research (C) (Grant no. 21K06495) from the Japan Society for the Promotion of Science (JSPS), AMED under Grant Number JP20lm0203012, 21lm0203004j0005, and 22ym0126806j0001, Nakatani Foundation Grant Program for Biomedical Engineering Research, Kowa Life Science Foundation, and the Program for the Advancement of Next Generation Research Projects (Type C) at Keio to Y. H. The authors thank Dr Naoko Iwasawa, Mr Masato Ishizeki, and Ms Yuzuka Kuronuma of Keio University for the advice on synthesizing cyanine dyes.

## Conflicts of interest

There are no conflicts to declare.

## Notes and references

- J. Wu, Z. Shi, L. Zhu, J. Li, X. Han, M. Xu, S. Hao, Y. Fan, T. Shao, H. Bai, B. Peng, W. Hu, X. Liu, C. Yao, L. Li and W. Huang, *Adv. Opt. Mater.*, 2022, **10**, 2102514.
- J. Yin, Y. Hu and J. Yoon, *Chem. Soc. Rev.*, 2015, **44**, 4619–4644.
- R. J. Iwatate, M. Kamiya and Y. Urano, *Chem. Eur. J.*, 2016, **22**, 1696–1703.
- Y. Urano, D. Asanuma, Y. Hama, Y. Koyama, T. Barrett, M. Kamiya, T. Nagano, T. Watanabe, A. Hasegawa, P. L. Choyke and H. Kobayashi, *Nat. Med.*, 2009, **15**, 104–109.
- M. Mihara, H. Hara, J. Araki, K. Kikuchi, M. Narushima, T. Yamamoto, T. Iida, H. Yoshimatsu, N. Murai, K. Mitsui, T. Okitsu and I. Koshima, *PLoS One*, 2012, **7**, e38182.
- C. Zhang, S. Wang, J. Xiao, X. Tan, Y. Zhu, Y. Su, T. Cheng and C. Shi, *Biomaterials*, 2010, **31**, 1911–1917.
- R. C. Gilson, R. Tang, A. Som, C. Klajer, P. Sarder, G. P. Sudlow, W. J. Akers and S. Achilefu, *Mol. Pharmaceutics*, 2015, **12**, 4237–4246.
- T. Myochin, K. Kiyose, K. Hanaoka, H. Kojima, T. Terai and T. Nagano, *J. Am. Chem. Soc.*, 2011, **133**, 3401–3409.
- A. Kurutos, Y. Shindo, Y. Hiruta, K. Oka and D. Citterio, *Dyes Pigm.*, 2020, **181**, 108611.
- B. Tang, F. Yu, P. Li, L. Tong, X. Duan, T. Xie and X. Wang, *J. Am. Chem. Soc.*, 2009, **131**, 3016–3023.
- K. Kiyose, S. Aizawa, E. Sasaki, H. Kojima, K. Hanaoka, T. Terai, Y. Urano and T. Nagano, *Chem. Eur. J.*, 2009, **15**, 9191–9200.
- L. He, W. Lin, Q. Xu, M. Ren, H. Wei and J.-Y. Wang, *Chem. Sci.*, 2015, **6**, 4530–4536.
- K. Miki, K. Kojima, K. Oride, H. Harada, A. Morinibu and K. Ohe, *Chem. Commun.*, 2017, **53**, 7792–7795.
- X. Xie, G. A. Crespo and E. Bakker, *Anal. Chem.*, 2013, **85**, 7434–7440.
- S.-n. Uno, M. Kamiya, T. Yoshihara, K. Sugawara, K. Okabe, M. C. Tarhan, H. Fujita, T. Funatsu, Y. Okada, S. Tobita and Y. Urano, *Nat. Chem.*, 2014, **6**, 681–689.
- M. Kamiya, D. Asanuma, E. Kuranaga, A. Takeishi, M. Sakabe, M. Miura, T. Nagano and Y. Urano, *J. Am. Chem. Soc.*, 2011, **133**, 12960–12963.
- M. Sakabe, D. Asanuma, M. Kamiya, R. J. Iwatate, K. Hanaoka, T. Terai, T. Nagano and Y. Urano, *J. Am. Chem. Soc.*, 2013, **135**, 409–414.
- L. Yuan, W. Lin and Y. Feng, *Org. Biomol. Chem.*, 2011, **9**, 1723–1726.
- C. Yue, P. Liu, M. Zheng, P. Zhao, Y. Wang, Y. Ma and L. Cai, *Biomaterials*, 2013, **34**, 6853–6861.
- F. G. Bordwell, J. A. Harrelson, Jr. and T. Y. Lynch, *J. Org. Chem.*, 1990, **55**, 3337–3341.
- Y. Ando, Y. Homma, Y. Hiruta, D. Citterio and K. Suzuki, *Dyes Pigm.*, 2009, **83**, 198–206.
- X. Xie, J. Zhai, Z. Jarolímová and E. Bakker, *Anal. Chem.*, 2016, **88**, 3015–3018.
- Q. Chen, J. Zhai, J. Li, Y. Wang and X. Xie, *Nano Res.*, 2022, **15**, 3471–3478.
- B. A. Webb, M. Chimenti, M. P. Jacobson and D. L. Barber, *Nat. Rev. Cancer*, 2011, **11**, 671–677.

